Article

Cell Metabolism

Pyruvate Kinase M2 Regulates Hif-1α Activity and IL-1β Induction and Is a Critical Determinant of the Warburg Effect in LPS-Activated Macrophages

Graphical Abstract

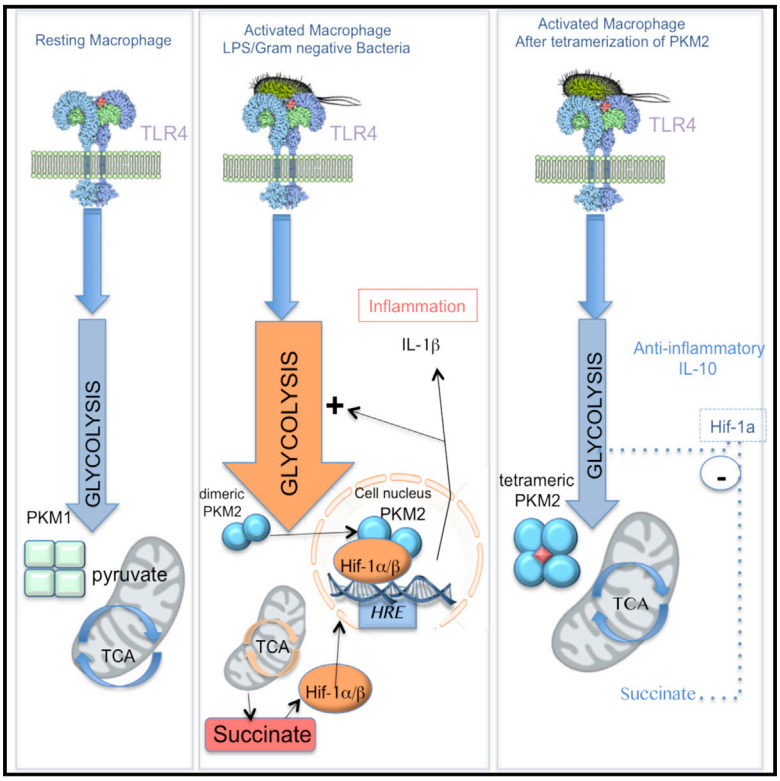

Highlights

- Tetramerization of PKM2 reverses the LPS-induced Warburg effect
- PKM2 plays a key role in stabilizing Hif-1α and regulates Hif-1α-dependent genes
- Tetramerization of PKM2 attenuates LPS-induced M1 macrophage traits
- PKM2 is a critical determinant of glycolytic reprogramming in macrophages

Authors

Eva M. Palsson-McDermott, Anne M. Curtis, ..., Ramnik J. Xavier, Luke A.J. O'Neill

Correspondence

laoneill@tcd.ie

In Brief

TLR4-activated macrophages switch their metabolism from oxidative phosphorylation to glycolysis to rapidly provide for the high energy and biosynthetic demands of infection or injury response. Palsson-McDermott identify PKM2 as a critical modulator of IL-1β production and the Warburg effect in LPS-activated macrophages, highlighting it as a target in cancer and inflammation.

Palsson-McDermott et al., 2015, Cell Metabolism *21*, 65–80
January 6, 2015
http://dx.doi.org/10.1016/j.cmet.2014.12.005

Cell Metabolism
Article

Pyruvate Kinase M2 Regulates Hif-1α Activity and IL-1β Induction and Is a Critical Determinant of the Warburg Effect in LPS-Activated Macrophages

Eva M. Palsson-McDermott,[1] Anne M. Curtis,[1] Gautam Goel,[2,3,4] Mario A.R. Lauterbach,[1] Frederick J. Sheedy,[5] Laura E. Gleeson,[5] Mirjam W.M. van den Bosch,[1] Susan R. Quinn,[1] Raquel Domingo-Fernandez,[1] Daniel G.W. Johnston,[1] Jian-kang Jiang,[7] William J. Israelsen,[6] Joseph Keane,[5] Craig Thomas,[7] Clary Clish,[4] Matthew Vander Heiden,[6,8] Ramnik J. Xavier,[2,3,4] and Luke A.J. O'Neill[1,*]

[1]School of Biochemistry and Immunology, Trinity Biomedical Science Institute, Trinity College Dublin, Dublin 2, Ireland
[2]Centre for Computational and Integrative Biology, Massachusetts General Hospital, Boston, MA 02114, USA
[3]Gastrointestinal Unit and Centre for the Study of Inflammatory Bowel Disease, Massachusetts General Hospital and Harvard Medical School, Boston, MA 02114, USA
[4]Broad Institute of Harvard University and Massachusetts Institute of Technology, Cambridge, MA 02142, USA
[5]Department of Clinical Medicine, School of Medicine, Trinity College, Dublin 2, Ireland
[6]Koch Institute for Integrative Cancer Research, Massachusetts Institute of Technology, Cambridge, MA 02142, USA
[7]National Institutes of Health (NIH), Chemical Genomics Centre, National Centre for Advancing Translational Sciences, NIH, Bethesda, MD 20892, USA
[8]Dana-Farber Cancer Institute, Harvard Medical School, Boston, MA 02215, USA
*Correspondence: laoneill@tcd.ie
http://dx.doi.org/10.1016/j.cmet.2014.12.005

SUMMARY

Macrophages activated by the TLR4 agonist LPS undergo dramatic changes in their metabolic activity. We here show that LPS induces expression of the key metabolic regulator Pyruvate Kinase M2 (PKM2). Activation of PKM2 using two well-characterized small molecules, DASA-58 and TEPP-46, inhibited LPS-induced Hif-1α and IL-1β, as well as the expression of a range of other Hif-1α-dependent genes. Activation of PKM2 attenuated an LPS-induced proinflammatory M1 macrophage phenotype while promoting traits typical of an M2 macrophage. We show that LPS-induced PKM2 enters into a complex with Hif-1α, which can directly bind to the IL-1β promoter, an event that is inhibited by activation of PKM2. Both compounds inhibited LPS-induced glycolytic reprogramming and succinate production. Finally, activation of PKM2 by TEPP-46 in vivo inhibited LPS and *Salmonella typhimurium*-induced IL-1β production, while boosting production of IL-10. PKM2 is therefore a critical determinant of macrophage activation by LPS, promoting the inflammatory response.

INTRODUCTION

Insights into the critical role of metabolic reprogramming in host defense and inflammation have recently emerged (Krawczyk et al., 2010; O'Neill and Hardie, 2013). In macrophages activated with the TLR4 agonist LPS, there is a high demand for biosynthetic precursors for proteins, lipids, and nucleic acids as well as increased energy demand. These events are required for the cells to respond to infection or tissue injury during inflammation. The metabolic changes that occur resemble the well-described Warburg effect (also known as aerobic glycolysis) first reported in tumor cells (Altenberg and Greulich, 2004; Warburg, 1923). These alterations include increased glucose uptake, an elevated rate of glycolysis, and an upregulated pentose phosphate pathway in conjunction with a reduced level of oxidative phosphorylation via the tricarboxylic acid (TCA) cycle (Tannahill et al., 2013).

Increased levels of the TCA cycle intermediate succinate as a consequence of this metabolic switch in highly glycolytic activated "M1" macrophages has revealed that succinate facilitates the signal leading to stabilization of hypoxia inducible factor-1α (Hif-1α) (Koivunen et al., 2007; Tannahill et al., 2013). This phenomenon, which has been described as "pseudo hypoxia," takes place when excess succinate is transported out of the mitochondria into the cytosol, where it can impair the activity of prolylhydroxylases (PHD), leading to stabilization and activation of Hif-1α (Selak et al., 2005). Hif-1α then positively regulates the proinflammatory cytokine IL-1β and other Hif-dependent genes including those encoding enzymes in glycolysis (Tannahill et al., 2013).

There is only limited information on the precise molecular determinants of this profound change in metabolism.

Numerous studies have reported a key role for PKM2 in aerobic glycolysis of tumors (Christofk et al., 2008; Mazurek et al., 2005; Tamada et al., 2012). Mammalian cells contain two PK genes. One encodes PKL and PKR, which are exclusively expressed in liver and red blood cells, respectively. The second gene encodes PKM1 and PKM2. These are generated by exclusive alternative splicing of the *Pkm* pre-mRNA (Chen et al., 2012; Takenaka et al., 1991). In glycolysis, pyruvate kinase is the rate-limiting enzyme that converts phosphoenolpyruvic acid (PEP) to pyruvate, a reaction that in differentiated tissue is mediated by

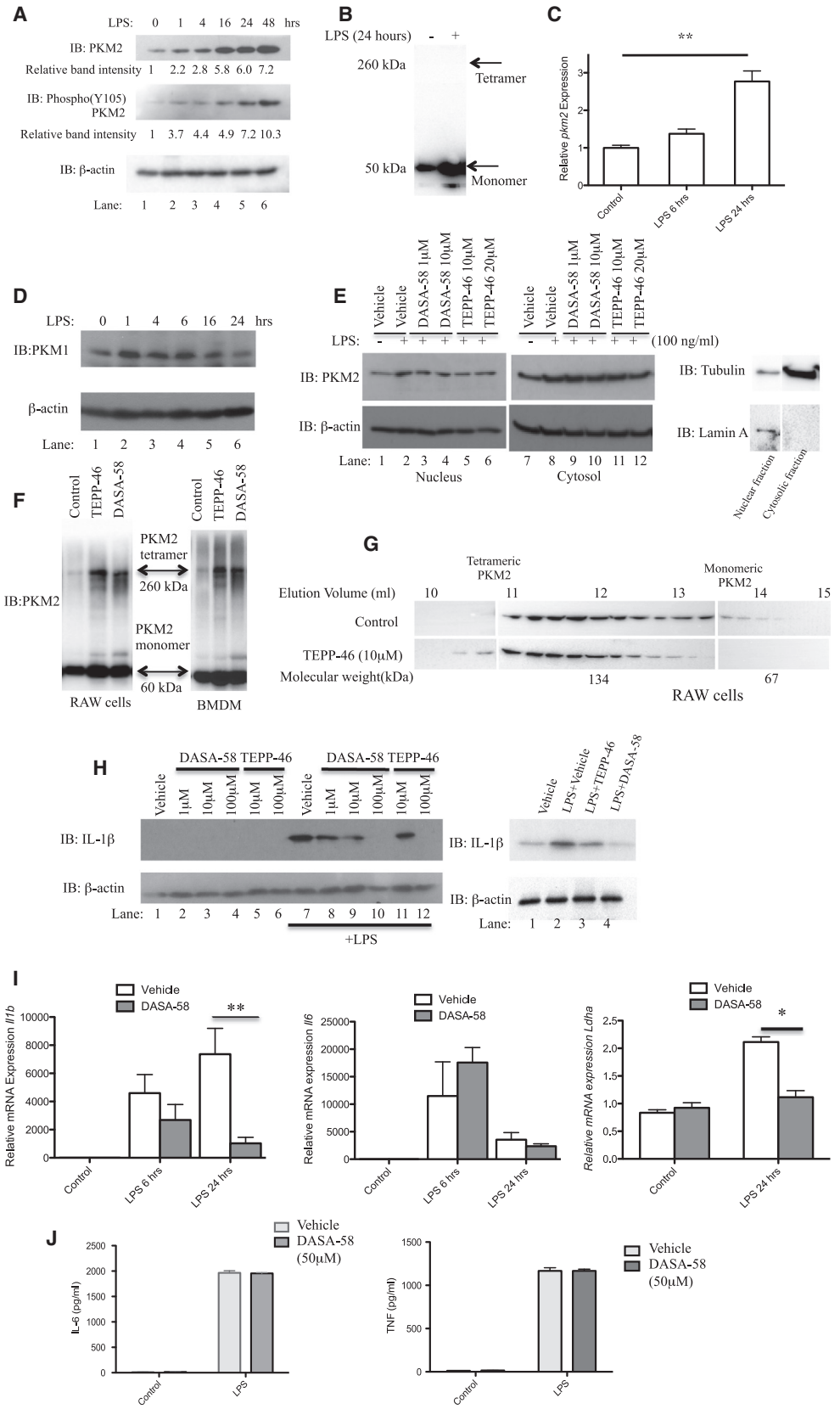

(legend on next page)

the enzymatically active isoform PKM1. PKM2 on the other hand is upregulated in tumors (Altenberg and Greulich, 2004) and exists primarily as an enzymatically inactive monomer or dimer. The PKM2 dimer can translocate to the nucleus, where it will interact with Hif-1α and regulate expression of numerous proglycolytic enzymes (Luo et al., 2011), an event that is dependent on ERK1/2 activity and regulated by Jumoji C domain-containing dioxygenase (JMJD5) (Wang et al., 2014; Yang et al., 2012). Other nuclear functions of dimeric PKM2 include the ability to act as a protein kinase, activating transcription of *mek5* through phosphorylation of STAT3 (Gao et al., 2012), as well as promoting β-catenin translocation, leading to expression of cyclinD1 and c-*myc* (Yang et al., 2011). Current evidence indicates that nuclear PKM2 thereby drives the Warburg effect in tumors (Yang and Lu, 2013).

The enzymatic pyruvate kinase activity of PKM2 can be allosterically triggered endogenously by fructose-1,6-bisphosphate (FBP), serine, and succinylaminoimidazolecarboxamide ribose-5′-phosphate (SAICAR) (Chaneton et al., 2012; Jurica et al., 1998; Keller et al., 2012). PKM2 can also be activated using the highly specific small-molecule activators DASA 58 and TEPP-46 (Anastasiou et al., 2012). These will bind PKM2-promoting tetramers to form, leading to an enzyme with a high pyruvate kinase activity, allowing PKM2 to mediate the last step of glycolysis by promoting the flux through glycolysis.

We provide evidence here for PKM2 induction in response to LPS in macrophages. This event is required for macrophage activation by LPS and we identify PKM2 as a critical modulator of IL-1β production, macrophage polarization, glycolytic reprogramming, and Warburg metabolism in LPS-activated macrophages. PKM2 therefore presents itself as a therapeutic target in both cancer and inflammation.

RESULTS

Tetramerization of PKM2 Using Small-Molecule Activators Inhibits LPS-Induced Activation of Primary Bone Marrow-Derived Macrophages

We hypothesized that, similar to tumor cells, PKM2 would be required for Warburg metabolism in LPS-activated macrophages. LPS induced high levels of PKM2 in bone marrow-derived macrophages (BMDMs) up to 48 hr (Figure 1A). Disuccinimidyl suberate (DSS) crosslinking of lysates from LPS-treated BMDMs suggest that LPS-induced PKM2 is primarily of a monomeric configuration (Figure 1B). Furthermore, LPS strongly induced *Pkm2* mRNA expression (Figure 1C), with expression levels increasing approximately 2.8-fold after 24 hr of LPS.

Phosphorylation of PKM2 on Tyrosine 105 is indicative of monomer/dimer formation, as it prevents PKM2 tetramer configuration, further promoting the Warburg effect (Hitosugi et al., 2009). LPS-induced expression of PKM2 causes concurrent phosphorylation of Tyrosine 105 to an extent comparable or greater to the increased expression levels. This phosphorylation is evident after just 1 hr, with the strongest induction after 48 hr (Figure 1A, middle, 10.3-fold increase in relative band intensity). This phosphorylation event suggests that PKM2 in LPS-activated macrophages primarily forms an enzymatically inactive dimer or monomer. This is further supported by results from the crosslinking experiments shown in Figure 1B, where DSS crosslinked lysates from LPS-treated BMDMs failed to reveal any high molecular weight PKM2 complexes.

Since PKM1 is the second alternatively spliced gene product of the *Pkm* gene, we also examined protein expression of PKM1 in response to LPS. As shown in Figure 1D, PKM1 expression levels did not increase substantially in response to LPS but instead a slight decrease in PKM1 protein was observed after 24 hr of LPS, confirming that in relation to the *Pkm* gene, the effect of LPS is specific to PKM2.

In order to examine the functional relevance of PKM2 for LPS action, we next examined the effect of two highly specific small-molecule PKM2 activators, TEPP-46 and DASA-58. These tool compounds were used to probe PKM2 function. They promote the formation of active PKM2 tetramers, thereby boosting PKM2 enzymatic activity and limiting tumor growth in vivo (Anastasiou et al., 2012).

We confirmed the targeting of PKM2 by DASA-58 and TEPP-46 by assessing the effect of PKM2 activation on the subcellular localization of PKM2. As depicted in Figure 1E, LPS caused an increased expression level of PKM2 in the cytosol (compare lane 7 to lane 8) as well as in the nucleus (compare lane 1 to lane 2). However, driving PKM2 into tetramers using DASA-58 (compare lane 3-4 to lane 2) and TEPP-46 (compare lane 5-6 to lane 2) inhibited LPS-induced nuclear translocation. However, such reduction of PKM2 in the cytosolic fraction was not evident in response to either compound. Fractions from vehicle-treated samples were immunoblotted for Tubulin and Lamin A to control for preparation purity.

Since previous reports have established that PKM2 enters the nucleus as a dimer, we then carried out further DSS crosslinking

Figure 1. Tetramerization of LPS-Induced PKM2 in Primary BMDMs Inhibits the Hif-1α Targets IL-1β and Ldha

(A and C) LPS-stimulated BMDMs were assayed for expression of PKM2, Y105-phosphorylated PKM2, and β-actin by western blotting (A) and *Pkm2* mRNA by qRT-PCR (C).

(B) Crosslinking (500 μM DSS) and western blot of endogenous PKM2 in BMDMs ± LPS (24 hr).

(D) LPS did not significantly affect expression of PKM1 in BMDMs.

(E) BMDMs pretreated with ±DASA-58 or ±TEPP-46 as indicated, followed by LPS for 24 hr. Cytosolic and nuclear fractions were isolated and PKM2, β-actin, Lamin A, and Tubulin were detected by western blotting.

(F) DSS crosslinking and western blotting of PKM2 in BMDMs and RAW macrophages after treatment ±100 μM TEPP-58 or ± 50 μM DASA-46.

(G) RAW macrophages treated with ±10 μM TEPP-58 or DMSO (1 hr), followed by LPS. Protein separated by size exclusion chromatography and blotted for PKM2.

(H) BMDMs (left) or PECs (right) were pretreated ±DASA-58 or TEPP-46 (30 min), followed by stimulation with LPS for 24 hr. Cell lysates were analyzed for pro-IL-1β or β-actin expression by western blotting.

(I and J) *Il1b* (left), *Il6* (middle), and *Ldha* (right) mRNA (I) and IL-6 (left) and TNF (right) protein expression (J) were measured in BMDMs treated with ±DASA-58 and LPS for 6–24 hr. Data represent mean ± SEM, n = 3, $^{**}p < 0.01$.

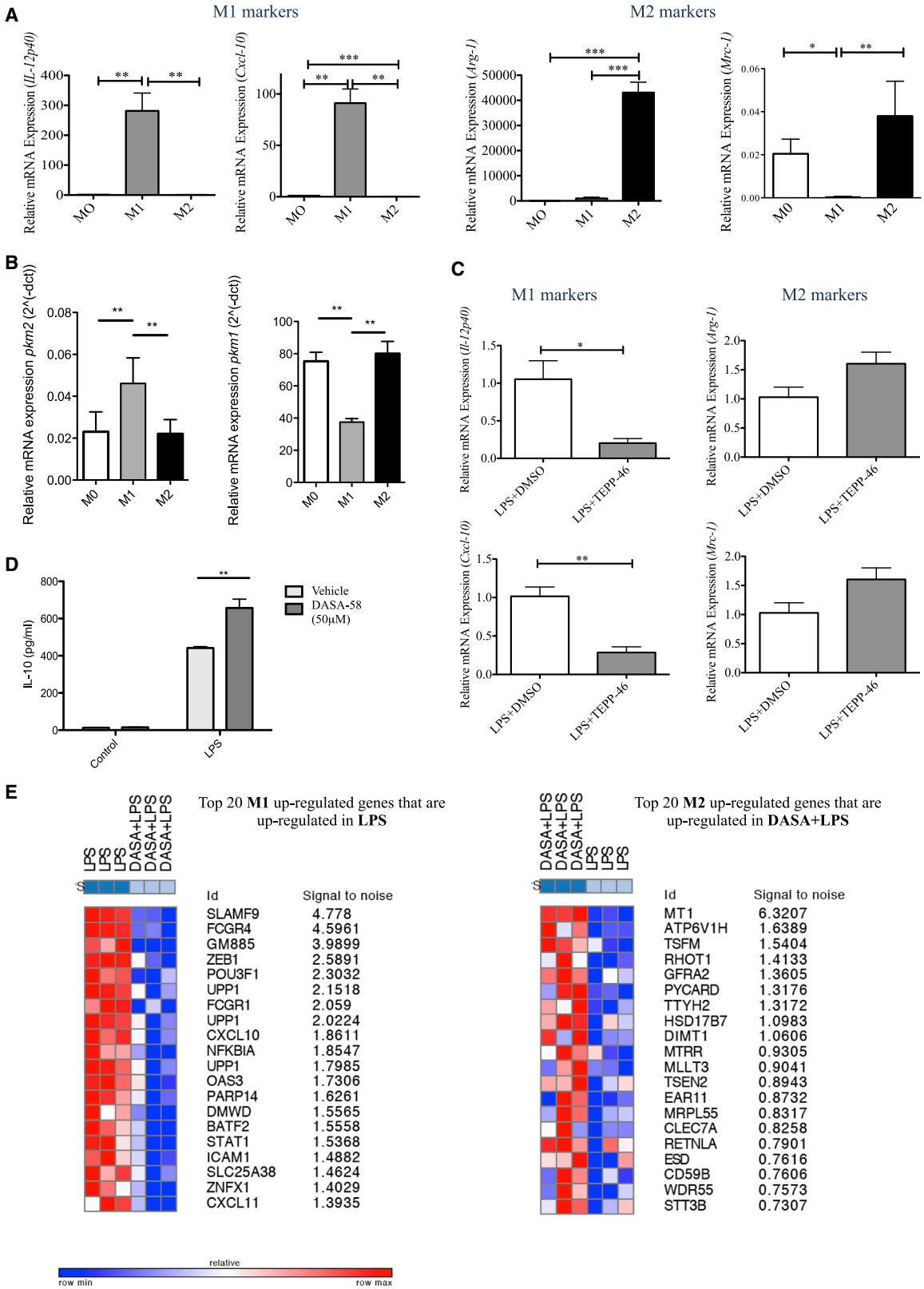

Figure 2. Activation of PKM2 Using TEPP-46 Attenuates the M1 Attributes of LPS-Activated BMDMs

BMDMs were stimulated with 100 ng/ml LPS or 20 ng/ml IL-4 for M1 and M2 polarization, respectively; 24 hr after stimulation RNA was extracted. (A) Left to right, expression of *il12-p40*, *cxcl-10*, *arginase-1*, and *mrc-1* were analyzed to assess differentiation into M1 and M2 macrophages.

(legend continued on next page)

studies in order to support a model for nuclear exclusion of PKM2 following treatment with our small-molecule activators. RAW cells as well as primary BMDMs (Figure 1F) were treated with TEPP-46 and DASA-58 as indicated. Lysates were cross-linked using DSS and endogenous PKM2 was subsequently detected. The blot clearly reveals a high molecular weight PKM2-containing complex of approximately 250 kDa following treatment with TEPP-46 and DASA-58, pointing to a tetramer formation of PKM2. In addition, lysates from RAW cells treated with TEPP-46 were separated through size exclusion using fast protein liquid chromatography (FPLC) (Figure 1G). Fractions collected were analyzed by western blotting detecting PKM2 and the result reveals a shift in the molecular weight of PKM2 with the appearance of a band corresponding to approximately 250 kDa (Figure 1G, elution volume 10–11 ml) and a reduction of the smaller molecular weight complexes (elution volume 13–14), again suggesting a tetrameric formation of endogenous PKM2 following TEPP-46 treatment.

We know from a previous study that LPS-induced transcription of the proinflammatory cytokine IL-1β is an event closely linked to the Warburg metabolism of activated macrophages (Tannahill et al., 2013). Hence, we next examined the effect of activation of LPS-induced PKM2 using TEPP-46 and DASA-58 on the production of pro-IL-1β in activated BMDMs and peritoneal cells (PECs). As shown in Figure 1H, DASA-58 and TEPP-46 inhibited the induction of pro-IL-1β in LPS-activated BMDMs. Both compounds also inhibited LPS-induced pro-IL-1β in PECs (Figure 1H). As shown in Figure 1I, activation of PKM2 using DASA-58 also inhibited LPS-induced expression of *Il1b* mRNA but importantly had no effect on LPS-induced *Il6* mRNA levels. PKM2 activation also significantly inhibited LPS-induced expression of the Hif-1α target gene *Ldha*. Furthermore, LPS-induced IL-6 and TNF protein expressions (Figure 1J) were unaffected by activation of PKM2 consistent with these cytokine responses not directly requiring Warburg metabolism (Tannahill et al., 2013).

To further examine the effects of the specific small-molecule PKM2 activator in an unbiased fashion, we undertook a whole-genome transcriptomics analysis of LPS and LPS+DASA-58-treated BMDMs. We identified a signature set of 100 genes (Figure S1 available online, Table S1) for which the activation of PKM2 induced a markedly distinct response from that observed during LPS treatment alone. A general enrichment analysis of this gene set for biological pathways and processes (using MetaCore) identified significant regulation in predominantly immune response pathways (Tables S2 and S3). These included Interferon signaling, FcγR-mediated phagocytosis, and IL4 signaling. To examine specifically for signatures of metabolic pathways, we analyzed enrichment of metabolic networks and found 48 pathways to be significantly enriched (FDR < 0.05) with glycolysis being the top ranking metabolic pathway (Table S4). The key glycolytic enzymes underlying this signature are PFKP, ALDOC, and TPI1, all three of which directly regulate the levels of FBP in this pathway. Phosphofructokinase (PFKP), which catalyzes the irreversible conversion of fructose-6-phosphate to FBP, is relatively downregulated by activation of PKM2, whereas the enzymes downstream of this metabolite, namely ALDOC and TPI1, are significantly upregulated by DASA-58. This suggested that we would expect to find significantly lower levels of FBP metabolite during PKM2 activation compared to LPS stimulation alone. To assess candidate transcription factors that are likely perturbed by activation of PKM2, we analyzed the signature set for enrichment of target genes of known transcription factors (TFs). We found enrichment for several interferon-associated factors (IRF1, IRF8, ISGF3) as well as NRF2 and Hif-1α among the top ten candidate TFs (Table S5). Several of the well-known targets of HIF1α, such as Vimentin, Plaur (uPAR), Stap1 (Art-27), Sort1, and PFKP, were either downregulated or not expressed when BMDMs were stimulated with LPS in the presence of DASA-58.

These results suggest that activation of PKM2 in macrophages inhibited LPS-induced expression of proglycolytic and Hif-1α-dependent genes.

Activation of PKM2 Attenuates LPS-Induced M1 Macrophage Polarization in BMDMs

To further investigate the effect of activation of PKM2 on the pro- or anti-inflammatory phenotype of activated macrophages, we set up polarizing conditions to generate M0 (undifferentiated), M1 (classically activated), or M2 (alternatively activated) macrophages as described. Figure 2A validates the polarizing conditions showing an upregulation of the markers *Interleukin-12 p40* (*Il12p40*) and *C-X-C chemokine 10* (*Cxcl-10*) in M1 macrophages and an increased expression of *Arginase-1* (*Arg-1*) and *Mannose Receptor C, type 1* (*Mrc-1*) during M2 polarizing conditions. We next measured expression of PKM2 in these distinct macrophage populations and as Figure 2B shows, PKM2 expression is upregulated in M1 macrophages. In addition, we see a clear downregulation of PKM1 mRNA in these M1 macrophages.

In order to examine the effect of our tool compounds on the expression of M1 and M2 signature gene subsets, we next treated LPS-activated M1 macrophages with TEPP-46. As seen in Figure 2C, the expression of the M1 markers *Il12p40* and *Cxcl-10* are significantly downregulated following TEPP-46 treatment. Similarly, although not significant, we consistently observed a boost in the expression of the M2 markers *Arg-1* and *Mrc-1* by TEPP-46 in M1-polarized macrophages.

Interestingly, activation of PKM2 boosted LPS-induced expression of the anti-inflammatory M2 cytokine Interleukin-10 (IL-10) in BMDMs (Figure 2D), further supporting an attenuation of the M1 phenotype after activation of PKM2 in favor of a more M2-like macrophage.

(B) Expression of *pkm2* (left) and *pkm1* (right) was measured for each polarizing condition.

(C) BMDMs were pretreated with 100 μM TEPP-46 or DMSO (1 hr), followed by LPS (24 hr). RNA was extracted and expression of *il12-p40*, *cxcl-10*, *arginase-1*, and *mrc-1* was analyzed.

(D) IL-10 expression measured in supernatants from BMDMs ± DASA-58 (50 μM, 30 min) followed by LPS (24 hr). Data represent mean ± SEM, n = 3, $^{**}p < 0.01$.

(E) Transcriptomics data set profile GSE53053 used to identify genes that were significantly up- or downregulated in M1 or M2 polarizing conditions (two-tail two-sample t test; nominal p value ≤ 0.05, absolute log2-fold-change ≥ 2-fold). A chi-square test was performed to identify sets of up- or downregulated genes with significant patterns from microarray data (Figure S1) comparing LPS+DASA-58 to LPS-treated macrophages.

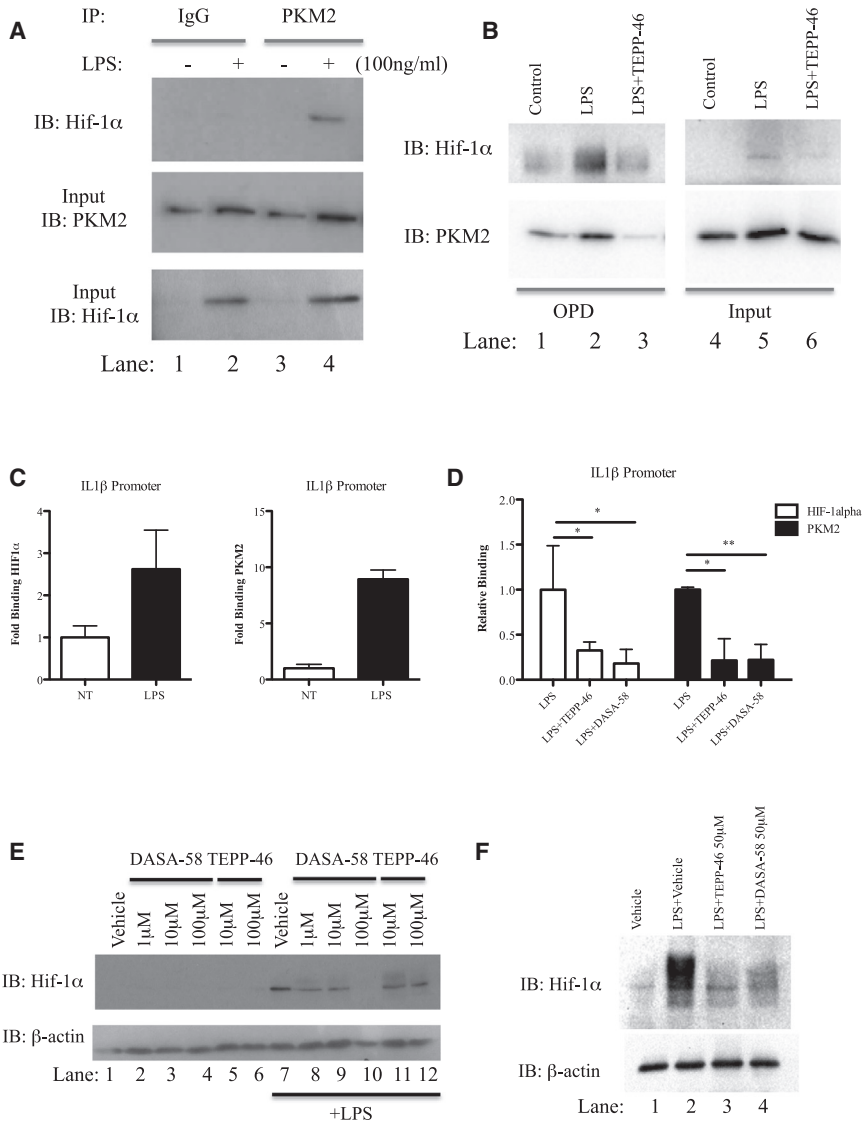

Figure 3. Dimeric/Monomeric PKM2 Is Required for LPS-Induced Binding of PKM2 and Hif-1α to the IL-1β Promoter

(A) Immunoprecipitation of PKM2 in BMDMs treated with LPS (24 hr). Hif-1α measured by immunoblotting.

(B) BMDMs treated ±TEPP-46 (50 μM, 60 min) followed by LPS (24 hr) were lysed and an OPD assay was carried out using oligonucleotide spanning the HIF1α binding site on the IL1β promoter. Samples were probed for Hif-1α (top) and PKM2 (bottom). Representative of n = 3.

(C and D) ChIP-PCR using PKM2 and HIF-1α antibodies and primers specific for −300 position of *Il1b* in LPS-treated BMDMs (C, sequential) and BMDMs treated with TEPP-46/DASA-58 (30 min, 50 μM) and LPS (100 ng/ml, 24 hr) (D). ChIP data are calculated as percent of input, represented as fold binding ±SD for one representative experiment (n = 3).

(E) BMDMs or (F) PECs (right) (1×10^6 cells per ml) were pretreated with indicated doses of DASA-58 or TEPP-46 (30 min), followed by LPS (100 ng/ml, 24 hr). Hif-1α or β-actin expression was analyzed by western blotting.

This effect on expression of M1 and M2 markers, together with our observation that DASA-58 causes an increased expression of LPS-induced IL-10 suggests that activation of PKM2 in LPS-activated macrophages may help to dampen the proinflammatory phenotype of the cell.

LPS Promotes Binding of PKM2 and Hif-1α to the IL-1β Promoter

PKM2 has been shown to interact with Hif-1α and stimulate Hif-1α transactivation domain function and recruitment of p300 to the Hif Response Element (HRE) of Hif-1α target genes (Luo et al., 2011). Treatment of BMDMs with LPS for 24 hr increased the association of endogenous PKM2 with endogenous Hif-1α, as shown in Figure 3A.

In order to investigate binding of PKM2 to the Hif-1α-specific binding site of the IL-1β promoter, we next used two approaches. First we employed an oligo pull-down (OPD) assay where an oligonucleotide specific to the Hif-1α binding site of the IL-1β promoter (−408; Tannahill et al., 2013) was incubated with lysates from TEPP-46 and LPS-treated primary BMDMs as indicated (Figure 3B). These results reveal binding of PKM2 to the IL-1β promoter (bottom left). In addition, there is an increased binding of both PKM2 and Hif-1α to this promoter site in response to LPS (compare lane 2 to lane 1). Furthermore, tetramerization of PKM2 using TEPP-46 inhibits LPS-induced binding of PKM2 and Hif-1α to the IL-1β promoter (compare lane 3 to lane 2).

We extended our binding studies to include sequential chromatin immunoprecipitation (ChIP) assays. This technique allows us to simultaneously examine the endogenous binding of two

To conclusively establish whether addition of DASA-58 prior to LPS treatment of macrophages led to an attenuation of LPS-induced M1 traits and these cells becoming more M2-like, we first downloaded and analyzed a transcriptomics profile of bone marrow-derived macrophages treated with either IL4 or a combination of LPS+Interferon-γ (IFNγ) (GSE53053). Using this data set, we identified genes that were significantly up- or downregulated in either M1 or M2 polarizing conditions (two-tail two-sample t test; nominal p value $\leq$ 0.05, Absolute log2-fold-change $\geq$ 2-fold). Next, we used a chi-square test to assess which set of up- or downregulated genes showed significant patterns in our own microarray data (from Figure S1) comparing LPS+DASA-58-treated macrophages to LPS-treated cells. We found that genes upregulated in M1 cells were significantly upregulated by LPS treatment compared to LPS+DASA-58 (Figure 2E). In addition to this, genes upregulated in the M2 signature set were also enriched for genes upregulated by DASA+LPS compared to LPS alone but to a lesser extent.

transcription factors to chromatin in response to LPS. As seen in Figure 3C, LPS causes increased binding of endogenous Hif-1α to the IL-1β promoter (left), and interestingly after this sample was put through a second round of ChIP specific for PKM2 (right), we also saw an increased binding of endogenous PKM2 to the same copy of DNA in response to LPS. Furthermore, activation of PKM2 using TEPP-46 and DASA-58 caused significant inhibition of LPS-induced binding of both Hif-1α and PKM2 to the IL-1β promoter (Figure 3D).

A role for PKM2 in LPS-induced stability of Hif-1α was further verified by directly measuring LPS-induced Hif-1α protein as shown in Figure 3E, where DASA-58 and TEPP-46 inhibited the induction of Hif-1α protein in LPS-activated BMDMs. Both compounds also inhibited LPS-induced Hif-1α protein in peritoneal macrophages (Figure 3F).

PKM2 Activators Inhibit Glycolysis and the Accumulation of Succinate in LPS-Activated Macrophages

We next examined the metabolic consequences of PKM2 induction by LPS. We first investigated whether activation of PKM2 could inhibit LPS-induced glycolysis. BMDMs were treated with TEPP-46 and DASA-58 prior to LPS and extracellular acidification was monitored as shown in Figure 4A. LPS caused up to a 10-fold increase in glycolysis, which is markedly inhibited by both TEPP-46 and DASA-58. Neither TEPP-46 nor DASA-58 had a significant effect on oxidative phosphorylation as measured by oxygen consumption rate (data not shown).

One important consequence of LPS-induced metabolic reprogramming in macrophages is a buildup of succinate, which acts as an inflammatory signal contributing to increased Hif-1α dependent IL-1β expression (Tannahill et al., 2013). In agreement with a role for PKM2 in LPS action here, DASA-58 dramatically blocked LPS-induced succinate (Figure 4B).

We carried out a comprehensive metabolomic profiling of LPS-activated BMDMs in the presence or absence of DASA-58. We revealed a clear effect of PKM2 activation by DASA-58 in preventing LPS-induced glycolysis (Figure 4C and Table S6). LPS stimulation led to accumulation of upstream glycolytic intermediates, such as glucose-6-phosphate (G6P), FBP, dihydroxyacetone phosphate (DHAP), and phosphoglyceric acid (2-PG), and TCA cycle intermediates including malate, fumarate, and succinate (Figure 4C, left; all metabolites with significant accumulation [p value < 0.05] are shown in bold red text; those highlighted in yellow indicate upregulation following LPS stimulation). Activation of PKM2 prevented the accumulation of any of these glycolytic intermediates. These findings are consistent with the microarray results in which we found evidence to suggest depletion of FBP during activation of PKM2. Additionally, the pentose phosphate pathway intermediate Ribose 5-phosphate (R5P), was significantly accumulated in response to LPS (Figure 4C, left); however, this was alleviated by activation of PKM2 (right). Furthermore a significant upregulation in levels of purines and pyrimidines downstream of the pentose phosphate pathway (such as cytidine, inosine, and uridine) were observed in DASA-58-treated samples (Figure 4C, right), suggesting that PKM2 can somehow promote the process of pyridine and pyrimidine biosynthesis downstream of R5P. These metabolomic changes are consistent with DASA-58 activating PKM2, which would lead to a decrease in glycolytic and pentose phosphate pathway intermediates.

Isoform-Specific Deletion of PKM2 Inhibits LPS-Mediated Activation of Hif-1α and Expression of Hif-1α Target Genes in Macrophages

In order to confirm a role for PKM2 in LPS signaling, we next used BMDMs generated from mice carrying a conditional PKM2$^{fl/fl}$ allele allowing for Cre-recombinase-mediated deletion (Israelsen et al., 2013) and matched wild-type controls. Isolated BMDMs were treated with ±600 nM Tamoxifen for 72 hr prior to the experiment in order to excise the PKM2-specific *Pkm* Exon 10. *Pkm2* expression was successfully ablated (Figure 5A); however, as expected, *Pkm1* expression was compensatorily increased (Figure 5B). In addition, PKM2 protein levels were successfully reduced following treatment with Tamoxifen (Figure 5C, top panel, compare lanes 5 and 6 to lanes 7 and 8), whereas PKM1 protein was upregulated following Tamoxifen and LPS treatment compared to control (Figure 5C, second panel). LPS-induced Hif-1α protein was dramatically decreased in PKM2 knockout cells compared to mock-treated cells expressing PKM2 (Figure 5C, third panel; compare lane 2 to 4 in relation to lane 6 to 8). Furthermore, as a functional consequence of this, BMDMs lacking PKM2 displayed a significantly reduced mRNA expression level of the Hif-1α-responsive genes *Il1β* and *Ldha* in response to LPS (Figure 5D). In contrast, LPS-induced IL-6 and TNFα expression (Figure 5E) were comparable in Tamoxifen-treated versus mock-treated PKM2$^{fl/fl}$ BMDMs. This result clearly pointed to the requirement for PKM2 in the activation of HIF1α in response to LPS.

Using BMDMs generated from PKM2$^{fl/fl}$ mice, we measured the rate of glycolysis in response to LPS. Macrophages with diminished expression of PKM2 displayed a reduced rate of glycolysis in response to LPS compared to cells with an intact PKM2 gene (depicted in Figure 5F). Furthermore, BMDMs with an impaired PKM2 gene exhibit an increased rate of oxidative phosphorylation as measured by oxygen consumption rate (OCR) (Figure 5F). However, although as expected LPS causes a reduction in OCR in PKM2+/+ cells (Tannahill et al., 2013), the same inhibitory effect was still observed in BMDMs derived from PKM2$^{-/-}$ cells (data not shown). Taken together, these results point to a key role for PKM2 in LPS-induced glycolysis.

In order to control for off-target effects of TEPP-46 and DASA-58, Tamoxifen-treated BMDMs derived from conditional PKM2$^{fl/fl}$-deficient mice were treated with TEPP-46 prior to LPS and relative IL-1β expression was measured (Figure 5G). LPS-induced *Il1b* expression was attenuated in PKM2-ablated cells, with no further inhibitory effect observed following pretreatment with TEPP-46 or DASA-58.

Activation of PKM2 Using TEPP-46 Modulates the Anti-*Mycobacterium tuberculosis* Response of Macrophages

To extend our investigations into PKM2 beyond LPS to an infectious agent that utilizes TLRs other than TLR4, we next examined a bacterial pathogen, *Mycobacterium tuberculosis* (*Mtb*). As the main causative agent of tuberculosis, *Mtb* signals mainly through TLR 2, 6, and 9 (Bafica et al., 2005; Means et al., 1999).

Resting BMDMs were stimulated with FSL-1, a ligand for TLR2 and TLR6 or the TLR9 ligand CpG (Figure 6A) for up to 24 hr.

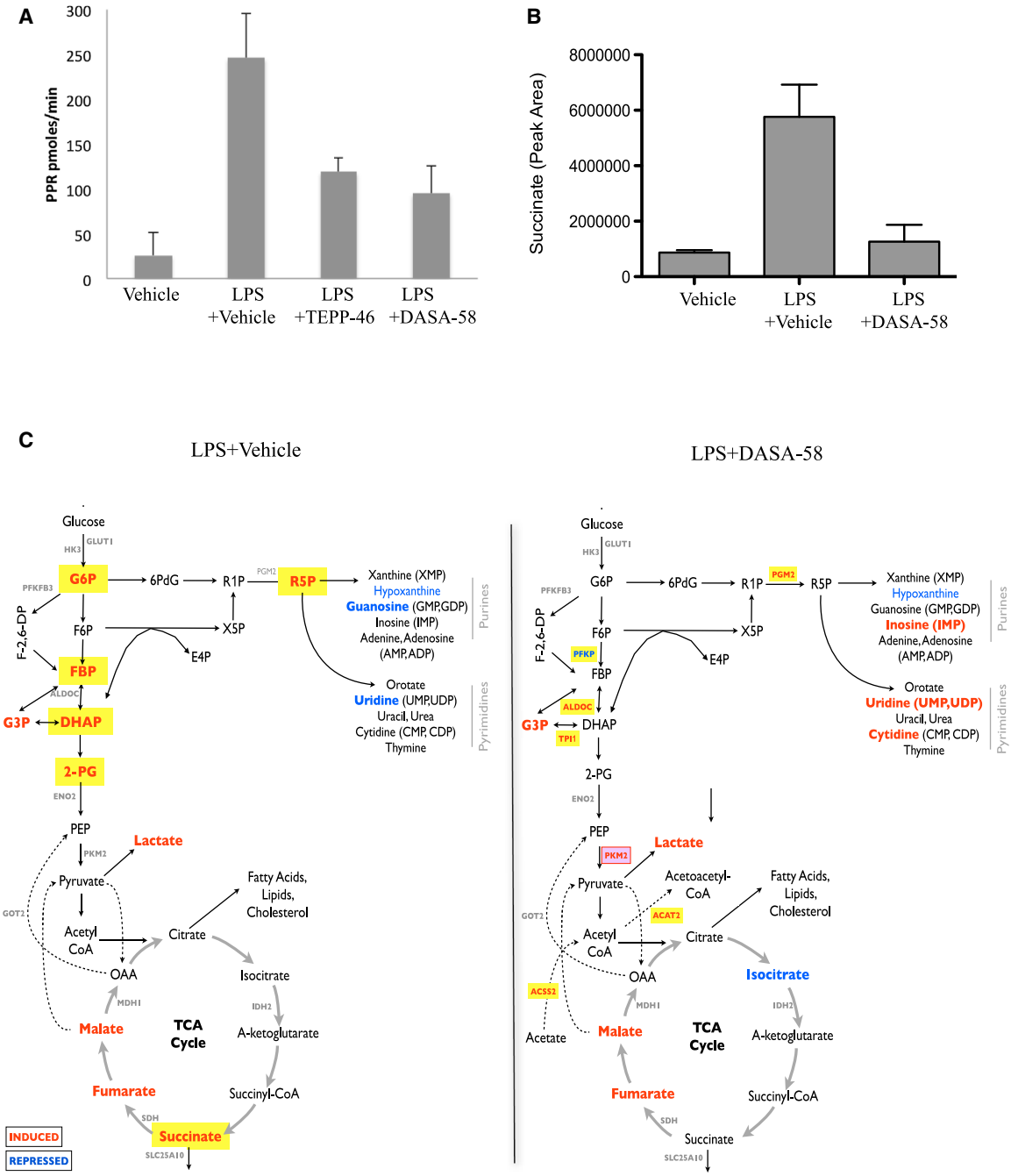

Figure 4. Activation of PKM2 Counteracts LPS-Induced Excessive Rate of Glycolysis and Restores Cellular Levels of Succinate

(A) Rate of glycolysis in BMDMs treated ±TEPP-46 (50 μM) or DASA-58 (50 μM) ±LPS.

(B) Succinate levels in LPS-treated BMDMs ± DASA-58 (50 μM) represented as relative abundance.

(C) Schematic map illustrating key metabolites and genes that were significantly enhanced (red) or inhibited (blue) in LPS-treated (100 ng/ml, 24 hr) BMDMs ± 50 μM DASA-58. All metabolites with significant accumulation (p value < 0.05) are shown in bold red text. Those in yellow suggest upregulation specific to LPS stimulation. Statistical analysis performed on three separate experiments. Metabolites with p value < 0.05 and fold-change > 10% were deemed to be statistically significant.

Similarly to LPS, these ligands induced expression of PKM2 both at protein level (Figure 6A) and mRNA level (Figure 6B). In addition, both FSL-1 and CpG induced pro-IL-1β and Hif-1α protein expression (Figure 6A). Activation of PKM2 using TEPP-46 significantly inhibited FSL-1 and CpG-induced *Il1b* mRNA expression (Figure 6C).

We next turned to intact heat-inactivated *Mtb* as a stimulus. Results from BMDMs treated with *Mtb* for 24 hr revealed an

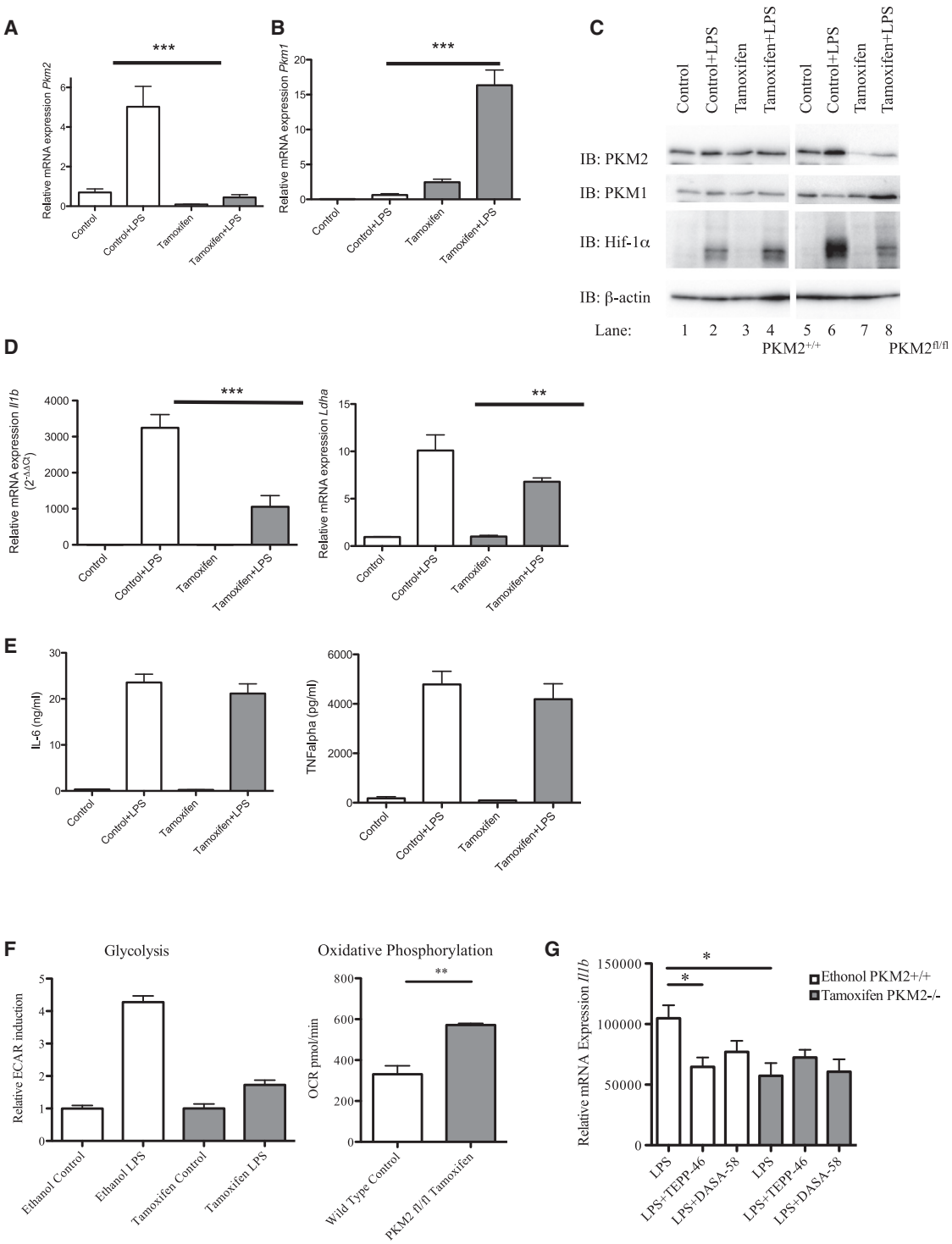

Figure 5. Inhibition of LPS-Induced Hif-1α and Hif-1α Target Genes in PKM2-Depleted BMDMs

(A–D) BMDMs from mice carrying a $PKM2^{fl/fl}$ allele and relative $PKM2^{+/+}$ controls were treated with ±600 nM Tamoxifen (72 hr), followed by LPS (24 hr). Relative mRNA expression levels of *Pkm2* (A), *Pkm1* (B), *Il1b*, and *Ldha* (D) were measured by qRT-PCR. PKM2, PKM1, Hif-1α, and β-actin protein expression was measured by western blotting (C).

(E) IL-6 and TNFα protein measured by ELISA, depicted as means ± SD of results from triplicate determinations for one representative experiment, n = 2.

(F) Rate of glycolysis (left) and oxidative phosphorylation (right) in ethanol- ($PKM2^{+/+}$) and Tamoxifen- ($PKM2^{-/-}$) treated LPS-activated BMDMs derived from $PKM2^{fl/fl}$ mice, measured as ECAR and OCR ± SD (n = 5).

(G) BMDMs derived from $PKM2^{fl/fl}$ mice treated with ethanol ($PKM2^{+/+}$) or Tamoxifen ($PKM2^{-/-}$) followed by TEPP-46 or DASA-58 (30 min) and LPS (24 hr) as indicated. The cells were lysed and expression of *Il1b* mRNA was determined by qRT-PCR.

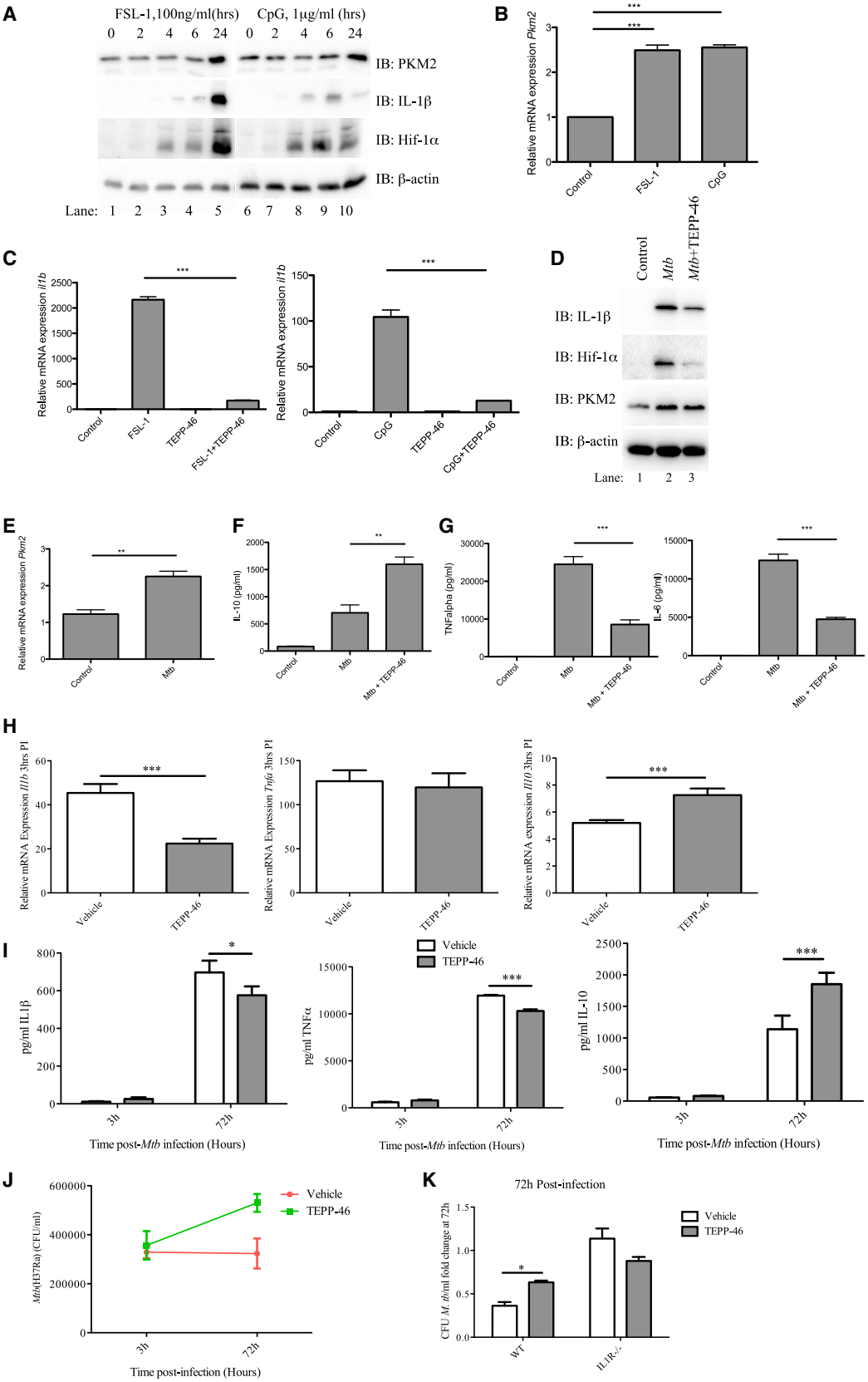

(legend on next page)

upregulation of PKM2 protein (Figure 6D, third panel, compare lanes 1 and 2) as well as PKM2 mRNA (Figure 6E). In addition, TEPP-46 inhibited *Mtb*-induced pro-IL-1β and Hif-1α protein, (Figure 6D), as well as TNFα and IL-6 (Figure 6G), while significantly boosting *Mtb*-induced IL-10 (Figure 6F). This result indicates an important role for PKM2 in innate immune host responses originating from Toll-like receptors other than TLR4.

In a model of macrophage infection using live *Mtb* (strain H37Ra), TEPP-46 inhibited *Mtb*-induced *Il1b* mRNA levels, boosted *Mtb*-induced levels of *Il10* mRNA, and had no effect on levels of *Tnf* (Figure 6H). In addition, *Mtb*-induced IL-1β, but also TNFα, protein levels were inhibited by TEPP-46, whereas IL-10 protein was significantly increased by activation of PKM2 (Figure 6I).

While no significant differences were observed in bacterial uptake 3 hr postinfection, Figure 6J shows an increased level of intracellular bacteria at 72 hr postinfection in TEPP-46-treated, *Mtb*-infected BMDMs compared to *Mtb* infection alone. These data are consistent with IL-10 promoting pathogen persistence by contributing to *Mtb* phagosome maturation block (O'Leary et al., 2011).

As illustrated in Figure 6K, BMDMs derived from IL-1 type I receptor knockout mice when infected with *Mtb* display an increased bacterial load compared to wild-type cells, with no effect of TEPP-46, demonstrating the requirement for intact IL-1 autocrine signaling for efficient bacterial killing.

Activation of PKM2 Results in Increased Bacterial Dissemination in a *Salmonella typhimurium* Model of Infection

Upregulation of aerobic glycolysis in macrophages during endotoxemia plays a central part in the pathology of this disease (Tannahill et al., 2013). TEPP-46, but not DASA-58, is pharmacokinetically validated in vivo (Anastasiou et al., 2012). TEPP-46 efficacy as a PKM2 activator had been verified using key in vitro assays as discussed above. To investigate the protective effects of activation of PKM2 in vivo, we gave mice TEPP-46 prior to an LPS challenge in a model of sepsis. As shown in Figure 7A, this dramatically reduced levels of pro-IL-1β produced by the peritoneal cells of these mice, compared to LPS treatment alone. Furthermore, administration of TEPP-46 prior to LPS resulted in animals expressing less IL-1β in the serum (Figure 7B), while IL-6 levels were the same as in the LPS-alone-treated animals (Figure 7C). As observed in BMDMs, serum levels of IL-10 (Figure 7D) were greatly increased in animals given TEPP-46 prior to the LPS challenge, compared to the control group. This suggests that activation of PKM2 in vivo counteracts the inflammatory effects of LPS, most likely through inhibiting Warburg metabolism.

In order to further investigate the effect of TEPP-46 in a model of infection, we used *Salmonella typhimurium* (strain UK-1) in an in vitro model of infection. BMDMs were treated with TEPP-46 prior to infection with *S. typhimurium*; 4 hr postinfection intracellular bacterial load was counted (Figure 7E). Cells treated with TEPP-46 displayed an increased bacterial load probably due to decreased bacterial killing by the cell.

We next used *S. typhimurium* in an in vivo model of infection. Similarly to the results obtained from the LPS-induced model of sepsis, peritoneal cells from mice treated in vivo with TEPP-46 prior to infection with *S. typhimurium* display a significant reduction in IL-1β protein expression levels (Figure 7F) 2 hr postinfection. Serum levels of IL-6 and IL-18 (Figure 7G) remained unchanged in TEPP-46-treated animals compared to the control group; however, once again serum levels of IL-10 were greatly enhanced in animals that were given TEPP-46 prior to infection.

In order to measure bacterial dissemination, mice were intraperitoneally infected with *S. typhimurium* and sacrificed 24 hr postinfection. Livers and spleens were extracted and log colony-forming units (CFUs)/organ were determined as illustrated in Figure 7H. The bacterial load in the spleens and in the livers in animals given TEPP-46 prior to infection was significantly increased. This is likely to be due to decreased bacterial killing due to the ability of TEPP-46 to inhibit IL-1β production while simultaneously promoting production of anti-inflammatory IL-10.

DISCUSSION

Inflammatory immune cells, such as "M1" type macrophages, dendritic cells, or Th17 cells harbor many of the metabolic changes displayed by tumor cells. This allows the host immune system to support anabolic processes and meet the increased demand for biosynthetic precursors required for mounting an immune response. Central to the metabolic switch observed in tumors is PKM2, which we now demonstrate also plays a key role in the glycolytic switch occurring in LPS-activated macrophages. We demonstrate PKM2 upregulation and phosphorylation in an activated macrophage, with only a minor change in PKM1 protein expression. As LPS induces formation of a PKM2 and Hif-1α complex that can bind to the IL-1β promoter, this points to a role for PKM2 as an important regulator of

Figure 6. Activation of PKM2 Modulates Anti-Mycobacterial Macrophage Responses

(A and B) Cell lysates from FSL-1- and CpG- (24 hr) treated BMDMs were analyzed for PKM2, IL-1β, Hif-1α, or β-actin expression by western blotting (A) and *pkm2* mRNA by qRT-PCR (B).

(C) BMDMs pretreated with TEPP-46 (50 μM, 30 min) were activated using FSL-1 (100 ng/ml) and CpG (1 μg/ml) for 24 hr. *il1b* was analyzed by qRT-PCR.

(D–G) Expression levels of IL-1β, Hif-1α, PKM2, and β-actin protein (D), *pkm2* mRNA (E), IL-10 (F), TNFα, and IL-6 protein (G, left and right) were measured in BMDMs ± TEPP-46 (30 min) stimulated using heat-inactivated *Mtb*.

(H) BMDMs ± TEPP-46 (25 μM) were infected with live *Mtb* H37Ra (MOI 5 bacteria/cell, 3 hr) and gene expression of *Il1b* (left), *tnf* (middle), and *Il10* (right) mRNA analyzed (qRT-PCR). Data are mean ± SD for triplicate determinations, n = 2.

(I) BMDMs ± TEPP-46 (25 μM) were infected as above (3 and 72 hr). IL-1β (left), TNFα (middle), and IL-10 (right) production were measured in supernatants of infected cells.

(J) BMDMs from (I) were lysed and CFU/ml determined.

(K) BMDMs derived from wild-type or IL-1 type I receptor knockout cells were infected as for (H) above. Cells were lysed at 72 hr postinfection and CFU/ml determined. Depicted as means ± SD of results from triplicate wells for one representative experiment n = 2. *$p < 0.05$, **$p < 0.01$, ***$p < 0.001$ (two-way ANOVA with post hoc Bonferroni correction).

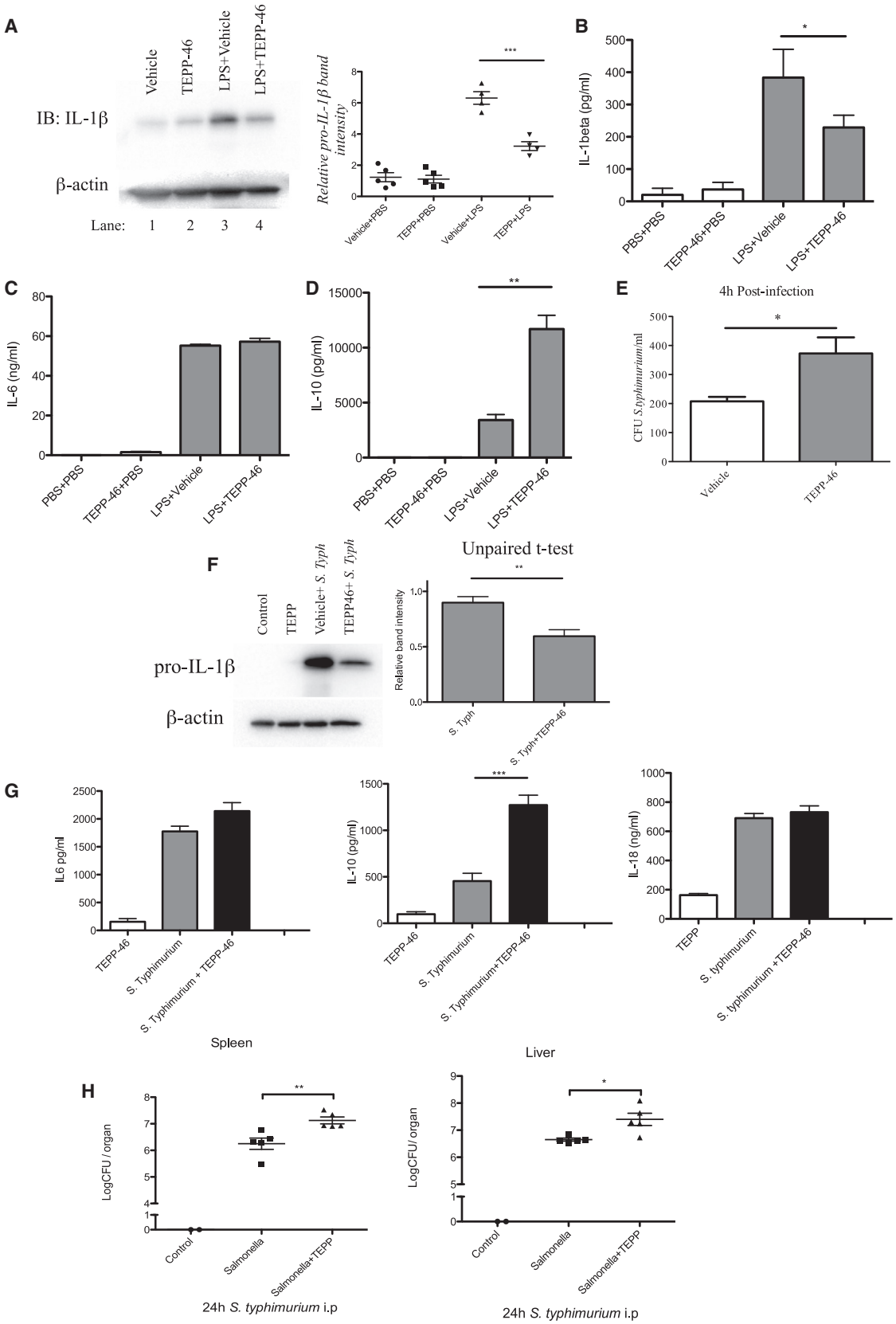

(legend on next page)

Hif-1α activity, and Hif-1α-dependent genes in host defense, as previously described in hypoxia and cancer where nuclear PKM2, with PHD3 acting as a cofactor, regulates the transcriptional activity of Hif-1α (Luo et al., 2011).

In addition, using isoform-specific PKM2 conditional knockout cells, we show that induction of PKM2 by LPS is critical for Hif-1α stabilization, in agreement with previous studies demonstrating a PKM2/Hif-1α complex targeting Hif-1α expression (Luo et al., 2011). Hif-1α will also be stabilized by succinate inhibiting PHDs, providing further regulation of Hif-1α.

Current data indicate that PKM2, when highly expressed, exists in an equilibrium of enzymatically inactive pyruvate kinase dimers (or monomers), which can translocate into the nucleus (Christofk et al., 2008; Hitosugi et al., 2009), and enzymatically active tetramers, which are retained in the cytosol (Mazurek et al., 2005). The pyruvate kinase activity of the tetramers can be regulated by the concentration of the naturally occurring upstream glycolytic intermediate FBP (Ashizawa et al., 1991; Jurica et al., 1998), serine (Chaneton et al., 2012), as well as by a multitude of posttranslational modifications (Wu and Le, 2013) including tyrosine phosphorylation. Activity is controlled by stabilizing or destabilizing the tetramer (Hitosugi et al., 2009). Tyrosine phosphorylation of PKM2 at residue 105 will inhibit the formation of a tetramer by dislodging the binding of FBP. This event has been shown to be important for the Warburg effect in hypoxia and cancer (Hitosugi et al., 2009). We have found that this also occurs in LPS-activated macrophages, reflecting the similarities in metabolic changes observed in cancer, and suggesting a role for PKM2 in the Warburg effect in macrophages. This role was confirmed using PKM2-activating compounds DASA-58 and TEPP-46. These well-characterized and highly specific compounds bind PKM2, which then forms a tight tetramer with PKM1-like kinetic properties, an event that is resistant to inhibition by tyrosine phosphorylation. In addition to relieving the buildup of glycolytic intermediates, evident from the higher pyruvate kinase activity of the PKM2 tetramer (Anastasiou et al., 2012), this process also prevents nuclear translocation and therefore decreases the expression of several Hif-1α target genes such as *Ldha* (Luo et al., 2011). We show that activation of PKM2 by DASA-58 or TEPP-46 forces PKM2 to take on a tetrameric form. This impairs the ability of the PKM2 and Hif-1α complex to bind to the Hif-1α motif in the promoter of the known Hif-1α target gene IL-1β (Peyssonnaux et al., 2007; Zhang et al., 2006), thereby inhibiting the transcriptional activity of Hif-1α and induction of IL-1β and conceivably other Hif-1α-dependent genes in response to LPS. This validates a role for dimeric/monomeric PKM2 in LPS action here. Interestingly, the effects of activating PKM2 also extend into changing the polarizing phenotype of a macrophage, with tetramerization of LPS-induced PKM2 in an M1 macrophage-promoting characteristics typical of the M2 phenotype. This implies that the activation of PKM2 is a potential therapeutic approach in inflammatory diseases.

Activation of PKM2 also inhibited induction of IL-1β and boosted IL-10 production in *Mtb*-infected macrophages promoting bacterial growth. This extended our observation beyond TLR4 and LPS to a bacterial pathogen that utilizes TLR2, TLR6, and TLR9.

We demonstrated the impact tetramerization of PKM2 on limiting the host immune response in vivo, by attenuating both LPS and *S. typhimurium*-induced IL-1β while boosting IL-10, leading to impaired clearance of infection evident from increased bacterial dissemination. Our results are in agreement with the study of Yang et al., who demonstrated that inhibition of PKM2 with shikonin prevented lethality in a model of septic shock, although the mechanism of shikonin is not fully understood (Yang et al., 2014).

We confirmed that LPS stimulation leads to accumulation of upstream glycolytic intermediates, such as G6P, FBP, DHAP, and 2-PG, and TCA cycle intermediates including succinate (Tannahill et al., 2013). Activation of PKM2 using DASA-58 dramatically reverts this glycolytic phenotype. Coupled results of metabolomics and microarray analysis further indicated PKM2-mediated metabolic reprogramming of activated macrophages. The data indicate a combination of transcriptional regulation of key enzymes to increase flux into lactate, divert metabolites into the pentose phosphate pathway, and thereby divert pyruvate away from the TCA cycle. These events are all prevented by PKM2 activation by DASA-58 and TEPP-46, which thereby prevent macrophage activation by LPS.

Another consequence of the metabolic changes in LPS-activated macrophages is an increase in succinate. Activation of PKM2 also limits this response and this will lead to Hif-1α destabilization. From our data, the effect of PKM2 activation in terms of pyruvate kinase activity on LPS-activated macrophages is therefore 3-fold. First, it will limit the nuclear function of PKM2 and decrease Hif-1α-dependent gene expression. Second, the decrease in succinate will further limit Hif-1α through stabilization and degradation. Finally, it will decrease levels of glycolytic and pentose phosphate pathway metabolites, thereby limiting biosynthesis. The increased pyruvate kinase activity of PKM2 will also increase the flux of pyruvate into the TCA cycle. This could explain the increase in IL-10 production, which in the case of M2 macrophage activity may require mitochondrial oxidative metabolism (Krawczyk et al., 2010). Precisely how PKM2 promotes IL-10 production requires further analysis.

Figure 7. Activation of PKM2 In Vivo Diminishes the Host Immune Response in LPS-Induced Sepsis and in an *S. typhimurium* Model of Infection

(A–D) Pro-IL-1β in PECs isolated from mice injected i.p. with TEPP-46 (50 mg/kg) or vehicle control (20% 2-Hydroxypropyl-β-cyclodextrin) for 1 hr, followed by PBS or 15mg/kg LPS for 2 hr (A). Left: one representative sample from each treatment group. Right: densitometry readings of pro-IL-1β western blots from five mice per group and treatment, normalized to β-actin. Serum levels of IL-1β (B), IL-6 (C), and IL-10 (D) from mice in (A). n = 5 for each group, mean ± SEM, $^{**}p < 0.01$.

(E–G) BMDMs were treated ±TEPP-46 (30 min, 25 μM), prior to infection with *S. typhimurium* UK-1 strain at an MOI of ten bacteria/cell (E). Bacterial numbers were assessed at 4 hr p.i. CFU/ml enumerated 4 hr after plating. Mice were injected ±TEPP-46 (50 mg/kg), 1 hr prior to infection with *S. typhimurium* (1×10^6 CFU, 2 hr). Pro-IL-1β from PECs was measured by western blotting (F), and serum levels of IL-6, IL-10, and IL-18 were measured by ELISA (G).

(H) Mice were infected as in (F), and sacrificed 24 hr postinfection. Livers and spleens were extracted and Log CFU/organ was determined (n = 5 per group, mean ± SEM, two-tailed t test).

PKM2 in its dimeric, catalytically less active form is therefore required for glycolytic reprogramming in response to LPS, most likely because of the role dimeric PKM2 plays in Hif-1α function.

In conclusion, we have revealed a role for PKM2 in LPS-induced activation of macrophages and in macrophages infected with *Mtb*, as well as in an in vivo *S.typhimurium* model of infection providing important insights into the Warburg-like metabolic changes in macrophages, likely to be very important for inflammation and infection. Targeting PKM2 in order to inhibit glycolysis or re-engaging mitochondrial oxidative metabolism in an overactive macrophage may provide novel therapeutic approaches for inflammatory diseases.

EXPERIMENTAL PROCEDURES

Reagents

TEPP-46 and DASA-58 were synthesized in accordance with published methods (Boxer et al., 2010; Jiang et al., 2010). LPSs used in vitro (100 ng/ml) and in vivo were *E. coli*, serotype EH100 (Alexis), and 055:B5 (Sigma-Aldrich). 4-hydroxytamoxifen (H7904) was from Sigma. The following antibodies were used: anti-PKM2 (3198), antiphospho-PKM2 (Tyr105), β-actin (4267) (all Cell Signaling Technologies), anti-IL-1β (R&D, AF401-NA), anti-HIF-1α (Novus, NB100-449), and anti-PKM1 (Novus, NBP2-14833). Dimethyl sulfoxide (DMSO) was used as vehicle control for TEPP/DASA in all in vitro assays.

Mice and Cell Culture

BMDMs and PECs were isolated from C57BL/6 mice from Harlan UK as previously described (Tannahill et al., 2013). All experiments were carried out with prior ethical approval from Trinity College Dublin Animal Research Ethics Committee. Cells were used at 1 × 10^6 cells/ml unless otherwise stated. Each "n" represents BMDM/PECs from individual mice.

BMDMs from mice carrying a $PKM2^{fl/fl}$ allele were previously described (Israelsen et al., 2013). Ablation of PKM2 was achieved by adding 600 nM 4-hydroxytamoxifen (Sigma H7904) on day 4 of macrophage differentiation, until 24 hr prior to experiment.

Western Blotting

Western blot analysis was carried out as previously described (Fitzgerald et al., 2001). Western blots were developed using autoradiographic film or using a Gel Doc EZ System gel imaging system, alternatively.

RNA Isolation and Gene Expression

RNA was transcribed using High-Capacity cDNA Reverse Transcription Kit (Applied Biosystems). For mRNA, 18 s ribosomal RNA or RPS18 gene were used as housekeeping controls. Relative quantitation values were calculated using the 2(-Delta Delta C(T)) method (Livak and Schmittgen, 2001).

Nuclear and Cytosolic Fractionation

Nuclear Extract Kit (Active Motif, 40010) was used according to manufacturer's recommendations; 20 μl of each fraction was separated by SDS-PAGE prior to western blotting.

Crosslinking

BMDMs or RAW 264.7 macrophages were treated with 50 μM TEPP-46, 20 μM DASA-58 or DMSO. Crosslinking was performed using 500 μM disuccinimidyl suberate (Thermo Scientific Pierce) for 30 min. Lysates were analyzed by western blot.

Size Exclusion Chromatography

We loaded 2–3 mg protein from RAW 264.7 ± 10 μM TEPP-58 or DMSO (1 hr), followed by 100 ng/ml LPS (24 hr) on a Superdex 200 10/300GL column (GE Healthcare) and eluted with 50 mM sodium phosphate, 150 mM NaCl (pH7.5). We took 250 μl fractions and analyzed them by SDS-PAGE and western blot.

ELISA

ELISAs were performed according to manufacturers' instructions. Kits used were IL-1β (DY401), IL-6 (DY406), IL-10 (DY417), TNFα (DY410), and IL-1β (MLB00C, in vivo), IL-10 (M1000B, in vivo) (all from R&D). Results are presented as mean ± SEM. Two-tailed t tests were carried out.

Microarray Profiling and Measurement of LC-MS

Microarray and metabolomics profiling were performed as described in Tannahill et al. (2013).

Statistical Analysis of Microarray Data

Statistical analysis of microarray data was carried out in MATLAB. Data were checked for correlation between replicates (>0.96 on average within groups). Probes without any gene assignments were removed and further filtered on the basis of having a variance, signal, or entropy less than tenth percentile of the entire dataset. Remaining probes were analyzed for statistically significant differences (fold-change > 25%) between three groups (two-tailed t test assuming equal variance). We identified 107 probes (100 genes) as statistically significant across the three groups. p values were corrected for multiple hypothesis testing by Benjamini-Hochberg's method to control false discovery rate at 25%.

Coimmunoprecipitation

BMDMs (±LPS, 24 hr) were lysed as previously described (Fitzgerald et al., 2001). PKM2 immune complexes were precipitated using anti-PKM2 antibody coupled to protein A/G PLUS agarose beads (Santa Cruz Biotechnology) for 2 hr at 4°C. Nonspecific rabbit IgG antibody was used for control. Immunoprecipitated proteins were visualized by western blotting using anti-PKM2 or Hif-1α antibodies respectively. Lysates were blotted for PKM2 and Hif-1α to control for input.

Affinity Purification with Biotinylated Oligonucleotides

Oligonucleotides for the HIF1α binding site on the IL1β promoter were annealed as described (Quinn et al., 2014) (forward, 5′BIO-GGT AGG CAC GTA GAT GCA CAC C-3′; reverse, 5′-GGT GTG CAT CTA CGT GCC TAC C-3′). BMDMs (0.5 × 10^6 cell/ml) were treated with DASA (50 μM) or TEPP (100 μM) for 1 hr prior to LPS (24 hr). Oligonuceotide pull-down was performed as previously described (Quinn et al., 2014).

Chromatin Immunoprecipitation

BMDMs (0.5 × 10^6 cell/ml) were treated ±DASA-58 or TEPP-46 (1 hr) prior to LPS treatment for 24 hr. ChIP was performed as previously described (Quinn et al., 2014; Tannahill et al., 2013). Lysates were incubated with primary antibodies; Anti-HIF-1-α antibody (Abcam, ab2185), negative control anti-IgG (Sigma, I5006), and positive control Pol II Antibody (Santa Cruz Biotechnologies [N20] sc-899). For Sequential ChIP, the precipitated HIF1α sample was reprobed for binding of PKM2 (2 hr incubation, 30 μl preblocked Protein A/G beads, 30 μl PKM2 D78AXP antibody [4053]). qRT-PCR was carried out using primers for the IL1β promoter consensus HIF1α binding site (−408), or the β-actin promoter as a positive control for Pol II binding (data not shown). Data are calculated as percent of input and represented by one experiment expressed as fold binding (n = 3, ± SD).

Extracellular Acidification and Oxygen Consumption Rate

XF24 Extracellular Flux analyzer (Seahorse Biosciences) was used. BMDMs were plated at 200,000 cells/well in XF24 plates overnight then ± 50 μM TEPP-46 or DASA-58 (1 hr), followed by LPS for 24 hr. Results were normalized to cell number and are represented as mean ± SEM.

Statistical Analysis of Metabolomics Data

Processed data was log transformed (base 2). Correlation between replicates were >0.94 on average within different treatment groups. Significance was assessed using a two-tailed t test (assuming equal variance) and metabolites with fold-change > 10% were selected. Metabolites scoring with nominal p value < 0.05 across any of the four comparisons were selected for further analysis.

Mycobacterium Tuberculosis Assays

Infections were carried out at an MOI of 5 *Mtb* H37Ra/macrophage. For RNA analysis, cells were lysed in Trizol Reagent (Invitrogen). ELISA results are shown as means ± SEMs for one representative experiment n = 2. *p < 0.05, **p < 0.01, ***p < 0.001 (two-way ANOVA with post hoc Bonferroni correction).

In Vitro Uptake Assay

Serial dilutions of lysates from BMDM ± TEPP-46 infected with *S. typhimurium* strain UK-1 (MOI 10 bacteria/cell) were quantified as CFU/ml. Data are shown as mean ± SEM for three independent infections.

Endotoxin-Induced and *S. typhimurium* In Vivo Model of Sepsis

Mice were treated ± TEPP-46 (50 mg/kg) or vehicle (20% 2-Hydroxypropyl-β-cyclodextrin) i.p. for 1 hr; 15 mg/kg of LPS, alternatively 1 × 10^6 CFU *S. typhimurium* was administered i.p.; 2 hr postinfection serum was isolated from whole blood and PECs were harvested.

To measure bacterial dissemination, we sacrificed mice infected as above 24 hr postinfection. Log CFU/liver alt spleen was determined.

SUPPLEMENTAL INFORMATION

Supplemental Information includes Supplemental Experimental Procedures, one figure, and six tables and can be found with this article online at http://dx.doi.org/10.1016/j.cmet.2014.12.005.

AUTHOR CONTRIBUTUTIONS

E.M.P.-M. designed and did experiments, analyzed data, and wrote the manuscript, L.A.J.O. conceived ideas, oversaw the project and cowrote the manuscript, A.M.C, M.A.R.L, L.E.G., F.J.S., M.W.M.v.d.B., S.R.Q., R.D.-F., and D.G.W.J. designed and did experiments and analyzed data, G.G. performed bioinformatics analysis of metabolomic profiling and Illumina micorarray and advised on manuscript, R.J.X. and C.C., provided advice, performed metabolomic profiling and Illumina micorarray, J.-k.J., W.J.I., C.T., and M.V.H., provided advice and reagents. L.E.G, F.J.S., and J.K. performed *Mtb* experiments.

ACKNOWLEDGMENTS

We thank Science Foundation Ireland, the European Research Council, the Health Research Board, European Community Seventh Framework Programme (FP7-2007-2013) under grant agreement No. HEALTH-14-2011-281608 'TIMER', Wellcome Trust, Baggot St Hospital Trust, and National Institutes of Health for funding.

Received: May 3, 2014
Revised: October 16, 2014
Accepted: December 13, 2014
Published: January 6, 2015

REFERENCES

Altenberg, B., and Greulich, K.O. (2004). Genes of glycolysis are ubiquitously overexpressed in 24 cancer classes. Genomics *84*, 1014–1020.

Anastasiou, D., Yu, Y., Israelsen, W.J., Jiang, J.K., Boxer, M.B., Hong, B.S., Tempel, W., Dimov, S., Shen, M., Jha, A., et al. (2012). Pyruvate kinase M2 activators promote tetramer formation and suppress tumorigenesis. Nat. Chem. Biol. *8*, 839–847.

Ashizawa, K., Willingham, M.C., Liang, C.M., and Cheng, S.Y. (1991). In vivo regulation of monomer-tetramer conversion of pyruvate kinase subtype M2 by glucose is mediated via fructose 1,6-bisphosphate. J. Biol. Chem. *266*, 16842–16846.

Bafica, A., Scanga, C.A., Feng, C.G., Leifer, C., Cheever, A., and Sher, A. (2005). TLR9 regulates Th1 responses and cooperates with TLR2 in mediating optimal resistance to Mycobacterium tuberculosis. J. Exp. Med. *202*, 1715–1724.

Boxer, M.B., Jiang, J.K., Vander Heiden, M.G., Shen, M., Skoumbourdis, A.P., Southall, N., Veith, H., Leister, W., Austin, C.P., Park, H.W., et al. (2010). Evaluation of substituted N,N'-diarylsulfonamides as activators of the tumor cell specific M2 isoform of pyruvate kinase. J. Med. Chem. *53*, 1048–1055.

Chaneton, B., Hillmann, P., Zheng, L., Martin, A.C., Maddocks, O.D., Chokkathukalam, A., Coyle, J.E., Jankevics, A., Holding, F.P., Vousden, K.H., et al. (2012). Serine is a natural ligand and allosteric activator of pyruvate kinase M2. Nature *491*, 458–462.

Chen, M., David, C.J., and Manley, J.L. (2012). Concentration-dependent control of pyruvate kinase M mutually exclusive splicing by hnRNP proteins. Nat. Struct. Mol. Biol. *19*, 346–354.

Christofk, H.R., Vander Heiden, M.G., Harris, M.H., Ramanathan, A., Gerszten, R.E., Wei, R., Fleming, M.D., Schreiber, S.L., and Cantley, L.C. (2008). The M2 splice isoform of pyruvate kinase is important for cancer metabolism and tumour growth. Nature *452*, 230–233.

Fitzgerald, K.A., Palsson-McDermott, E.M., Bowie, A.G., Jefferies, C.A., Mansell, A.S., Brady, G., Brint, E., Dunne, A., Gray, P., Harte, M.T., et al. (2001). Mal (MyD88-adapter-like) is required for Toll-like receptor-4 signal transduction. Nature *413*, 78–83.

Gao, X., Wang, H., Yang, J.J., Liu, X., and Liu, Z.R. (2012). Pyruvate kinase M2 regulates gene transcription by acting as a protein kinase. Mol. Cell *45*, 598–609.

Hitosugi, T., Kang, S., Vander Heiden, M.G., Chung, T.W., Elf, S., Lythgoe, K., Dong, S., Lonial, S., Wang, X., Chen, G.Z., et al. (2009). Tyrosine phosphorylation inhibits PKM2 to promote the Warburg effect and tumor growth. Sci. Signal. *2*, ra73.

Israelsen, W.J., Dayton, T.L., Davidson, S.M., Fiske, B.P., Hosios, A.M., Bellinger, G., Li, J., Yu, Y., Sasaki, M., Horner, J.W., et al. (2013). PKM2 isoform-specific deletion reveals a differential requirement for pyruvate kinase in tumor cells. Cell *155*, 397–409.

Jiang, J.K., Boxer, M.B., Vander Heiden, M.G., Shen, M., Skoumbourdis, A.P., Southall, N., Veith, H., Leister, W., Austin, C.P., Park, H.W., et al. (2010). Evaluation of thieno[3,2-b]pyrrole[3,2-d]pyridazinones as activators of the tumor cell specific M2 isoform of pyruvate kinase. Bioorg. Med. Chem. Lett. *20*, 3387–3393.

Jurica, M.S., Mesecar, A., Heath, P.J., Shi, W., Nowak, T., and Stoddard, B.L. (1998). The allosteric regulation of pyruvate kinase by fructose-1,6-bisphosphate. Structure *6*, 195–210.

Keller, K.E., Tan, I.S., and Lee, Y.S. (2012). SAICAR stimulates pyruvate kinase isoform M2 and promotes cancer cell survival in glucose-limited conditions. Science *338*, 1069–1072.

Koivunen, P., Hirsilä, M., Remes, A.M., Hassinen, I.E., Kivirikko, K.I., and Myllyharju, J. (2007). Inhibition of hypoxia-inducible factor (HIF) hydroxylases by citric acid cycle intermediates: possible links between cell metabolism and stabilization of HIF. J. Biol. Chem. *282*, 4524–4532.

Krawczyk, C.M., Holowka, T., Sun, J., Blagih, J., Amiel, E., DeBerardinis, R.J., Cross, J.R., Jung, E., Thompson, C.B., Jones, R.G., and Pearce, E.J. (2010). Toll-like receptor-induced changes in glycolytic metabolism regulate dendritic cell activation. Blood *115*, 4742–4749.

Livak, K.J., and Schmittgen, T.D. (2001). Analysis of relative gene expression data using real-time quantitative PCR and the 2(-Delta Delta C(T)) Method. Methods *25*, 402–408.

Luo, W., Hu, H., Chang, R., Zhong, J., Knabel, M., O'Meally, R., Cole, R.N., Pandey, A., and Semenza, G.L. (2011). Pyruvate kinase M2 is a PHD3-stimulated coactivator for hypoxia-inducible factor 1. Cell *145*, 732–744.

Mazurek, S., Boschek, C.B., Hugo, F., and Eigenbrodt, E. (2005). Pyruvate kinase type M2 and its role in tumor growth and spreading. Semin. Cancer Biol. *15*, 300–308.

Means, T.K., Wang, S., Lien, E., Yoshimura, A., Golenbock, D.T., and Fenton, M.J. (1999). Human toll-like receptors mediate cellular activation by Mycobacterium tuberculosis. J. Immunol. *163*, 3920–3927.

O'Leary, S., O'Sullivan, M.P., and Keane, J. (2011). IL-10 blocks phagosome maturation in mycobacterium tuberculosis-infected human macrophages. Am. J. Respir. Cell Mol. Biol. *45*, 172–180.

O'Neill, L.A., and Hardie, D.G. (2013). Metabolism of inflammation limited by AMPK and pseudo-starvation. Nature *493*, 346–355.

Peyssonnaux, C., Cejudo-Martin, P., Doedens, A., Zinkernagel, A.S., Johnson, R.S., and Nizet, V. (2007). Cutting edge: Essential role of hypoxia inducible factor-1alpha in development of lipopolysaccharide-induced sepsis. J. Immunol. *178*, 7516–7519.

Quinn, S.R., Mangan, N.E., Caffrey, B.E., Gantier, M.P., Williams, B.R., Hertzog, P.J., McCoy, C.E., and O'Neill, L.A. (2014). The role of Ets2 transcription factor in the induction of microRNA-155 (miR-155) by lipopolysaccharide and its targeting by interleukin-10. J. Biol. Chem. *289*, 4316–4325.

Selak, M.A., Armour, S.M., MacKenzie, E.D., Boulahbel, H., Watson, D.G., Mansfield, K.D., Pan, Y., Simon, M.C., Thompson, C.B., and Gottlieb, E. (2005). Succinate links TCA cycle dysfunction to oncogenesis by inhibiting HIF-alpha prolyl hydroxylase. Cancer Cell *7*, 77–85.

Takenaka, M., Noguchi, T., Sadahiro, S., Hirai, H., Yamada, K., Matsuda, T., Imai, E., and Tanaka, T. (1991). Isolation and characterization of the human pyruvate kinase M gene. Eur. J. Biochem. *198*, 101–106.

Tamada, M., Suematsu, M., and Saya, H. (2012). Pyruvate kinase M2: multiple faces for conferring benefits on cancer cells. Clin. Cancer Res. *18*, 5554–5561.

Tannahill, G.M., Curtis, A.M., Adamik, J., Palsson-McDermott, E.M., McGettrick, A.F., Goel, G., Frezza, C., Bernard, N.J., Kelly, B., Foley, N.H., et al. (2013). Succinate is an inflammatory signal that induces IL-1β through HIF-1α. Nature *496*, 238–242.

Wang, H.J., Hsieh, Y.J., Cheng, W.C., Lin, C.P., Lin, Y.S., Yang, S.F., Chen, C.C., Izumiya, Y., Yu, J.S., Kung, H.J., and Wang, W.C. (2014). JMJD5 regulates PKM2 nuclear translocation and reprograms HIF-1α-mediated glucose metabolism. Proc. Natl. Acad. Sci. USA *111*, 279–284.

Warburg, O. (1923). Metabolism of tumours. Biochem. Z. *142*, 317–333.

Wu, S., and Le, H. (2013). Dual roles of PKM2 in cancer metabolism. Acta Biochim. Biophys. Sin. (Shanghai) *45*, 27–35.

Yang, W., and Lu, Z. (2013). Nuclear PKM2 regulates the Warburg effect. Cell Cycle *12*, 3154–3158.

Yang, W., Xia, Y., Ji, H., Zheng, Y., Liang, J., Huang, W., Gao, X., Aldape, K., and Lu, Z. (2011). Nuclear PKM2 regulates β-catenin transactivation upon EGFR activation. Nature *480*, 118–122.

Yang, W., Zheng, Y., Xia, Y., Ji, H., Chen, X., Guo, F., Lyssiotis, C.A., Aldape, K., Cantley, L.C., and Lu, Z. (2012). ERK1/2-dependent phosphorylation and nuclear translocation of PKM2 promotes the Warburg effect. Nat. Cell Biol. *14*, 1295–1304.

Yang, L., Xie, M., Yang, M., Yu, Y., Zhu, S., Hou, W., Kang, R., Lotze, M.T., Billiar, T.R., Wang, H., et al. (2014). PKM2 regulates the Warburg effect and promotes HMGB1 release in sepsis. Nat. Commun. *5*, 4436.

Zhang, W., Petrovic, J.M., Callaghan, D., Jones, A., Cui, H., Howlett, C., and Stanimirovic, D. (2006). Evidence that hypoxia-inducible factor-1 (HIF-1) mediates transcriptional activation of interleukin-1beta (IL-1beta) in astrocyte cultures. J. Neuroimmunol. *174*, 63–73.